

# Numerical Investigation On Reduced Beam Web Section Moment Connections Under The Effect Of Cyclic Loading

Akbar Hassanipour<sup>1</sup>, Rohola Rahnavard<sup>2</sup>, Ali Mokhtari<sup>3</sup>, Najaf Rahnavard<sup>4</sup>

- 1- Assistant professor of Earthquake Engineering, Dep. of Civil Engineering, Jundi Shapour University of Dezful, Iran, Hassanipour@jsu.ac.ir
- 2- Structure Engineering, Dep. of Civil Engineering, Jundi Shapour University of Dezful, Iran, Rahnavard1990@gmail.com
- 3- Structure Engineering member of Iran Construction Engineering Organization, Andimeshl, Iran, 13arad90@gmail.com
- 4- Khuzestan province, the municipality of Mianruod, rahnavard.najaf@yahoo.com

**Abstract—** Recent earthquakes have shown that steel moment frame (SMF) with weld connections are so brittle. According to the studies conducted, great damages are due to the cracking of the weld between the beam flange and the column face and inducing concentrated stresses in this area. A useful approach to reduce the stress concentration at the panel zone could be the use of reduced beam web section connection. In this study, six moment connection have been modeled using ABAQUS computer program and compared with each other during cyclic behavior. The obtained result of this study showed that reduced beam web section connections is more ductile and will dissipate energy more than other systems and also translated plastic hinge from connection to the reduced area.

**Keywords—** Reduced web; Finite element; Dissipation energy; plastic hinge

## I. INTRODUCTION

Moment-resisting frames are frequently used in regions of high seismic risk to resist seismic force. The moment connections of the moment-resisting frame are designed to connect the beam flange to the column using a complete joint penetration (CJP) groove weld in the field. A typical beam to column connection detail of a moment connection prior to the 1994 Northridge earthquake is shown in Figure 1. Many connections, however, failed in a brittle manner during the Northridge earthquake [1,2]. Brittle fractures occurred at the beam to column joint, resulting from several factors such as stress concentration in weld access hole regions, initiating crack due to back-up bars at the beam bottom flanges, weld defects, and material deficiencies (Mahin and Miller 1998)[3,4,5]. To prevent the premature failure of the joint, various improved details have been proposed in the aftermath of the Northridge earthquake. Post-Northridge connections include reduced beam section connections and reinforced connections that enable the required performance to be developed under cyclic

loading (Lee CH 2002) [6]. Cheng and Chih Chen (2004) [7] demonstrated that reinforcing the connection with a single rib can reduce the concentration of stresses at the root of the weld access hole. Tsai and Chen (2002) and Jones et al. (2002) experimentally illustrated that RBS moment connections with moderately strong panel zones show appropriate performance. Moslehi Tabar and Deylami (2013)[8] considered a new detail and proposed that the RBS performance be enhanced by delaying beam buckling. The efficiency of the proposed detail was investigated by a large scale laboratory testing under cyclic loading. The results of their study showed that the proposed RBS connection had superior performance as compared with the conventional one. The proposed detail increased plastic rotation capacity of the conventional RBS connection. Rahnavard (2013) [10,11] have studied bolt and weld moment connections in both with and without reduced section. They made some models in Abaqus software and compared them to find that the RBS connections increase ductility of beam and panel zone and also will result in reduction of stress and plastic strain concentration at the interface of beam and column. Sang-Whan Han, Ki-Hoon Moon and Bozidar Stojadinovic (2009)(2010)[12,13,14] studied the design equations of RBS connections and found that RBS-B connection moment strength equation specified in FEMA-350 [15], consistently overestimates the actual strength of the RBS-B connections measured in tests and the reduction of beam sections according to FEMA-350 which maybe therefore insufficient to protect the RBS-B connections. This, in turn, may lead to RBS-B connection failure before a plastic hinge forms at the reduced beam section of the beam.

The present paper aims to obtain results of numerical modeling on six subassemblies moment connections. The main objectives include: (1) to make comparison between all type of reduced beam web on ductility; (2) to study the effect of reduced beam web on concentration stress, strain and equivalent plastic strain at integration point (PEEQ) in different zones; (3) to obtain the influence of reduced beam web on

dissipated energy by the whole model; (4) to consider the pane zone in all models.

## II. NUMERICAL STUDY

The analytical study involves developing finite element model of connections for the purpose of evaluating the effect of various parameters on connection behavior. Three-dimensional nonlinear finite element of 6 models were created using ABAQUS computer program. The geometry and boundary conditions of the simple connection were based on the test set up used in the experimental study (Chou. C. C, Kai. Y. C, 2010) [9] that are shown on Figure 2 Point-wise boundary conditions (a pin and a roller) were modeled using rigid plates (undeformable mesh regions) which were attached to both ends of the column. Lateral movement of the flanges of the beam was prevented from column face in the 3.5 m. The beam web reduced by three methods including reduced beam web height, circular and sinuous holes in beam web. Figure 3 shows six types of the analytical models. Grade 50 steel ASTM-572 was used for column and continuity plates and also ASTM-A36 and ER-70S-6 for beam and weld electrode respectively. The mechanical properties of all component materials are taken from the experimental specimens mentioned in Table 1. An combined (isotropic-linear kinematic) hardening rule with a Von Mises yielding criterion is applied to simulate the plastic deformations of the connection components. This is suitable for simulation of metal plasticity under cyclic loading [24].

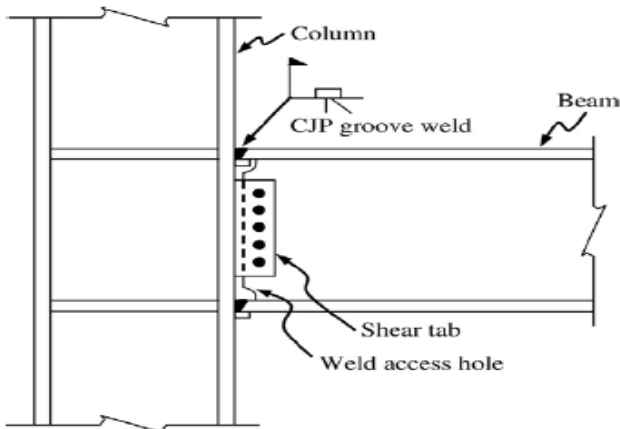


Figure 1: Typical pre-Northridge moment connection.

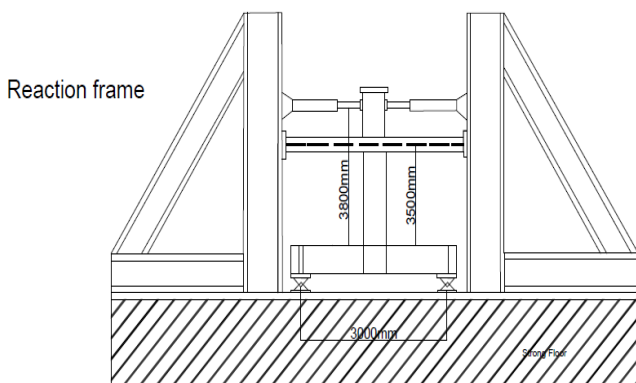


Figure 2: The specifications of specimens and test set-up.

A displacement-control loading was applied on the tip of the beam by imposing cyclic displacement based on SAC loading protocol (Figure 4). The beam tip displacement corresponding to the inter story drift angle of 0.01 rad. was 38 mm.

A typical three-dimensional finite element model of conventional connection is shown in Figure 5, where the models composed of eight-node brick elements with standard integration (element C3D8 in the ABAQUS element library). This element had 8 nodes and three degrees of freedom per node. With three elements through the thickness of column flanges and 5 elements and 6 elements used through the beam flanges and beam web, respectively. A better mesh was used to model the connection region and the beam and column region in the vicinity of the connected area.

To verify the analytical models, we modeled the conventional connection (model 1) tested by Chou C.C and Kai Y.C. As shown in Fig. 6, there is a close agreement between the experimental results obtained by Chou C.C and Kai Y.C. and our numerical results. It can be seen from the figure that the maximum moment at the surface between beam and column for experimental specimens and finite element model are 2210 kN.m and 2250 kN.m, respectively; which shows 2% differences in maximum values. Also the moment corresponding 4% radian connection rotate, for experimental and numerical result are 1650 kN.m and 1740 kN.m respectively which shows 6.5% differences. The comparison between the test and finite element analysis indicates that the finite element modeling procedures produce an accurate model, which should lead to accurate response prediction in the parametric study.

Table 1: MECHANICAL PROPERTY

Material	Application	Stress (Mpa)	Strain
ASTM-A572-Gr50	Column, Stiffness, Shear Plate	391	0.02
		525	0.06
		470	0.12
		391	0.24
ASTM-A36	Beam	288	0.013
		495	0.06
		390	0.12
		288	0.24
ER70S-6	Weld	469	0.025
		563	0.125
		510	0.245
		469	0.36

## III. DISCRIPTION OF ANALYSIS

### A. Stress Distribution

The Von Mises stress distributions for 0.06 radians inter story drift angle are shown in Figure 7 for all models. It can be seen that concentrated stress for all types of RBS models occurs in beams and for ordinary rigid connection (ORC) occurs in connection. In spite of the fact that in all RBS models, the panel zone

remained elastic, in ORC connection the panel zone had nonlinear behavior. As it can be seen, the local buckling of beam flange and web has occurred in 0.06 radians inter story drift. As indicated in Figure 7a, the brittle cracking may happen on weld area on ORC connection during the cyclic load.

### B. Plastic Strain Equivalent

The PEEQ index is defined as the plastic equivalent strain (PEEQ) divided by the yield strain  $\epsilon_y$  of the beam material, which represents the local strain demand (Chen and Chung 2005)[7]. The plastic equivalent strain is defined as below:

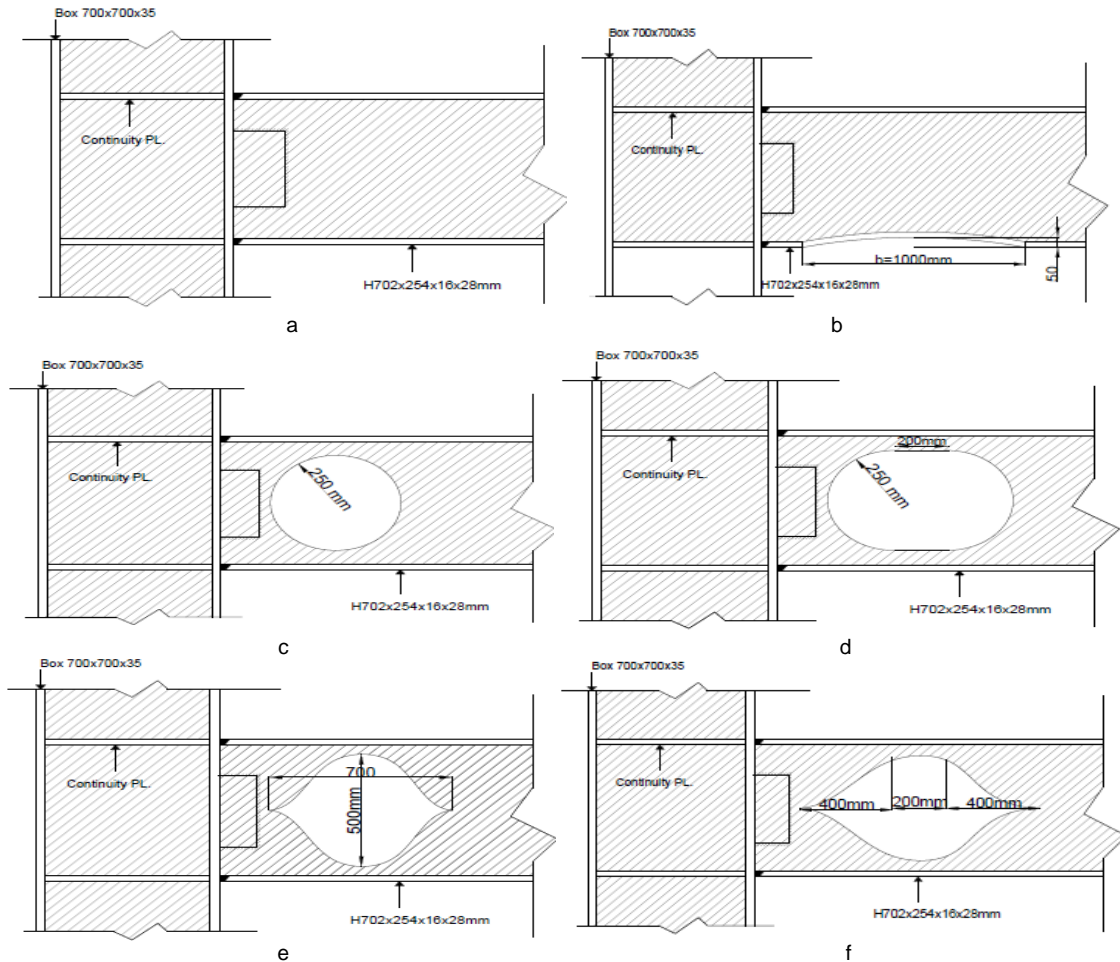


Figure 3: The details of connections. (a)ORC (b)RBS-W (c)RBS1-WH, (d)RBS2-WH (e)RBS1-S (f)RBS2-S

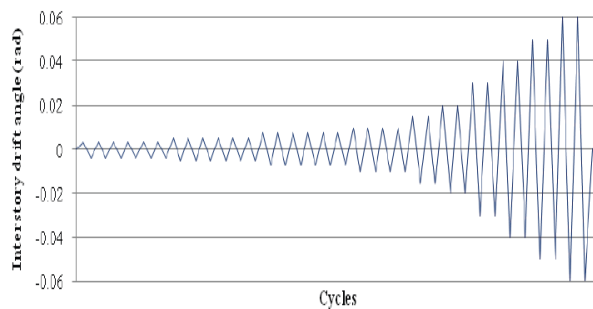


Figure 4:SAC loading protocol

$$PEEQ = \sqrt{\frac{2}{3} \epsilon_{ij} \epsilon_{ij}} \quad (1)$$

Where  $\epsilon_{ij}$  is the component of plastic strain in the direction specified by  $i$  and  $j$ .

The plastic equivalent strain (PEEQ) distributions for 0.06 radians inter story drift angle are shown in

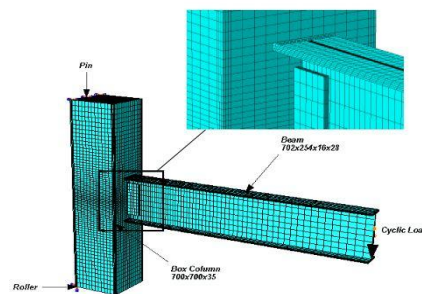


Figure 5: Finite element model.

Figure 8 for all models. It can be seen that concentrated strain for all types of RBS models occurs in beams and for ordinary rigid connection (ORC), it occurs in connection. As indicated in Figure 8, the plastic hinge occurs in weld groove between beam and column surface for ORC model. As it is evident, all types of reduced beam web section moment

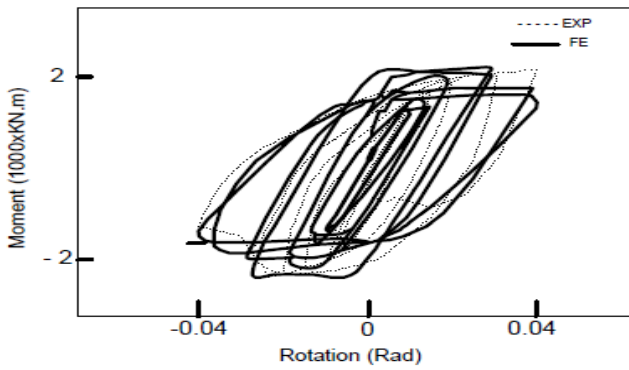


Figure 6: Comparison between the experimental and numerical hysteretic results

connections translate plastic hinge from the connection to the beam.

### C. Stress and Strain Concentrated

The results of finite element analyses are presented in the forms of the normalized longitudinal stress and PEEQ index. The longitudinal stress,  $\sigma_{11}$ , represents the normal stress in the beam flange and is normalized by the yield stress  $F_y$  of the beam material.

As described earlier, the PEEQ index is defined as the plastic equivalent strain (PEEQ) divided by the yield strain  $\epsilon_y$  of the beam material, which represents local strain demand (Chen and Chung 2005)[7].

The stress and plastic equivalent strain (PEEQ) distributions in two critical sections of the connection were studied. The selection of critical sections was based on the fracturing location in pre-Northridge moment connections. Figure 9 shows the critical sections, presented by lines running across the width of the beam flange. Line A is located at the complete joint penetration groove weld joining the beam and column flanges because many fractures have been found at this groove weld during the Northridge earthquake. Line B is located at the length of beam flange because that is the main purpose to translate concentrated stress and strain to from connection to beam. As it can be seen in Figure 10, just for ORC connection the magnitude of normal stress on weld area is greater than yield stress. This result shows that plastic hinge occurred in the connection for ordinary rigid connection and also plastic hinge occurred in the cutting regions for RBS models.

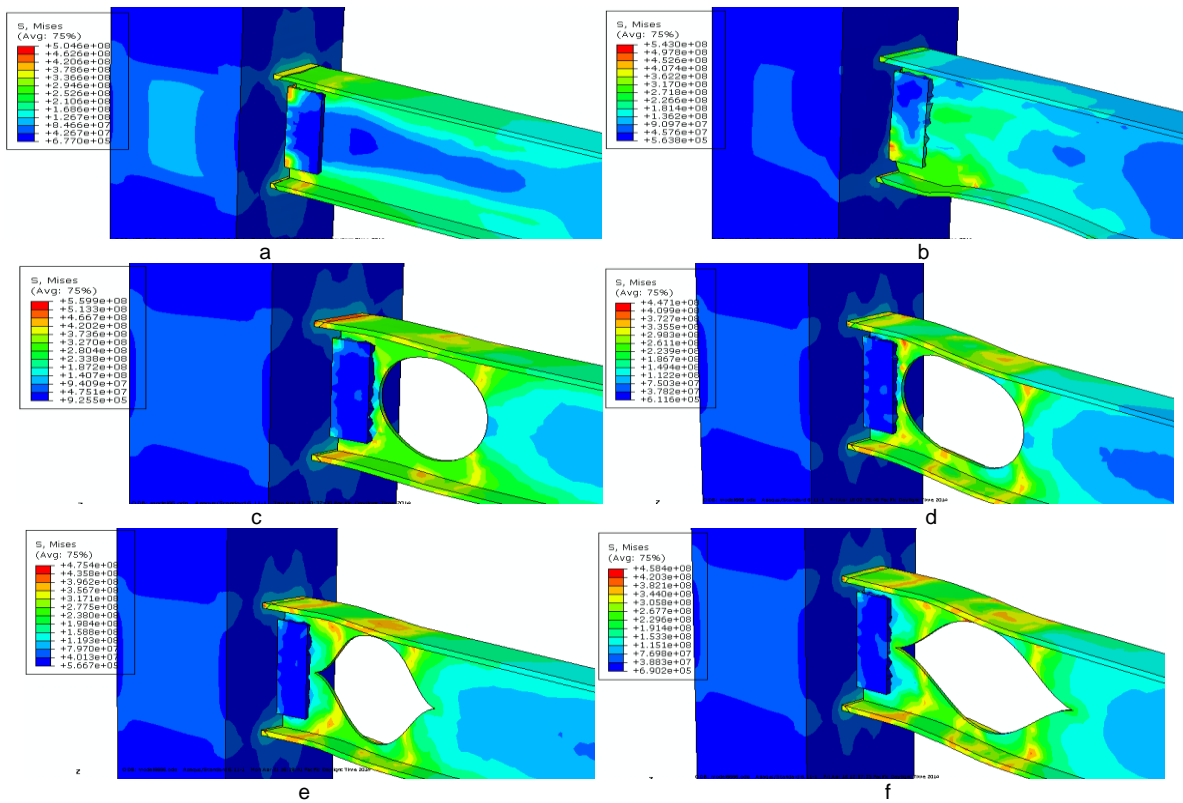
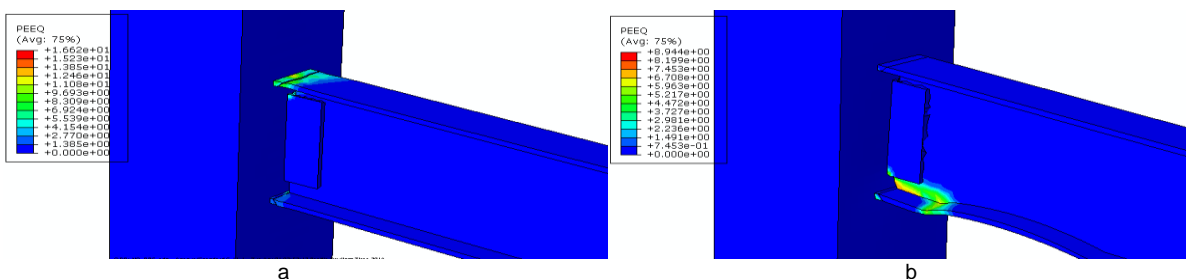


Figure 7: Von Mises distribution. (a)ORC (b)RBS-W (c)RBS1-WH, (d)RBS2-WH (e)RBS1-S (f)RBS2-S



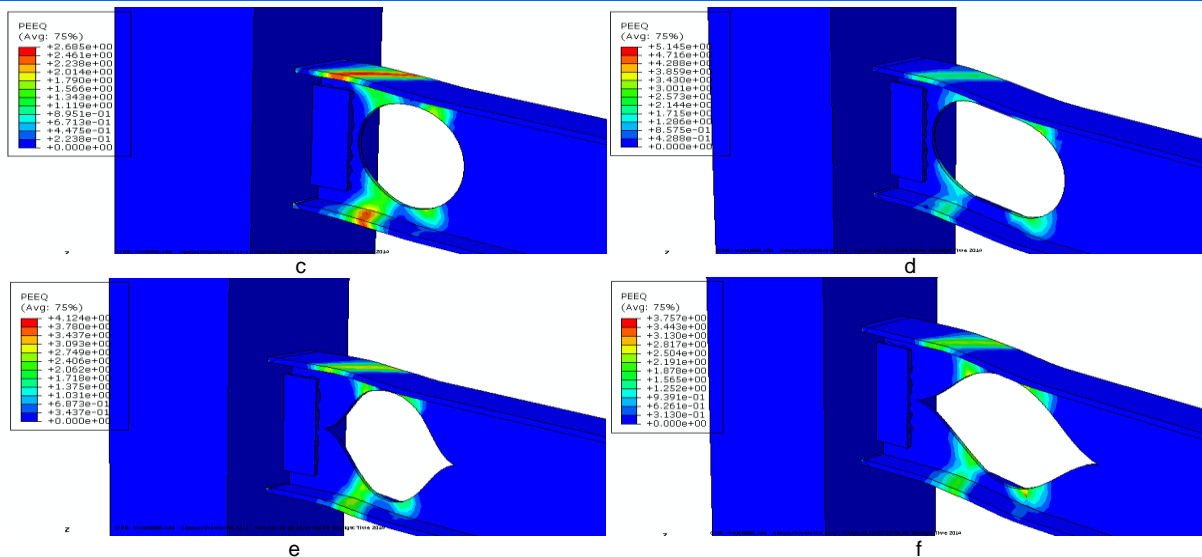


Figure 8: PEEQ Index. (a)ORC (b)RBS-W (c)RBS1-WH, (d)RBS2-WH (e)RBS1-S (f)RBS2-S

#### D. Cyclic Behavior

Moment–plastic rotation hysteretic responses of all models are shown in Figure 11. The moment was measured at the column face and the total beam rotation was computed by dividing the total beam tip displacement by the distance to the column face.

As it can be observed, all models have suitable hysteretic behavior. Hysteretic curves show that the strength of the connection is reduced due to beam local buckling. However, this strength degradation is not so important, since after the buckling, the strength of connection in all models is still more than plastic moment capacity of beams. Therefore, this connection can be classified as a full strength connection. As it can be observed from the hysteretic curves, all models have reached to 0.04 radians rotation, and the strength of connection at 0.04 radians rotation is more than 80 percent of the beam plastic moment capacity, (0.8Mp). Consequently, this connection satisfies the criteria of AISC Seismic Provisions (2005)[23] for special moment frame systems.

#### E. Connection Classification

The connections could be classified using moment–joint rotation curves. The joint rotation is considered as the summation of connection rotation and panel zone rotation.

Secant stiffness is computed using moment–joint rotation curves of models (Figure 13). Secant stiffness is defined as below:

$$K_s = M_s / \theta_s \quad (2)$$

$$M_s = F_y \times S \quad (3)$$

Where  $F_y$  is the yield stress of steel, and  $S$  is beam section modulus.

$\theta_s$  = joint rotation corresponding to  $M_s$  obtained from moment–joint rotation curves.

According to AISC Specifications for Structural Steel Buildings (2005), if  $KL/EI > 20$  the connections can be considered as fully restrained. Where,  $L$  and  $EI$  are length and bending rigidity of the beam respectively. Values of secant stiffness and  $K L/EI$  are presented in table 2 for all models. The value of  $L$  in this table is considered as equal to the length of beam in the frame between two columns which is twice the beam length in each side of column in selected subassemblies.

As it can be seen in table 1, all models are full restrained connection and also Secant stiffness magnitude in RBS-W and RBS2-S connections is bigger than that in other connections.

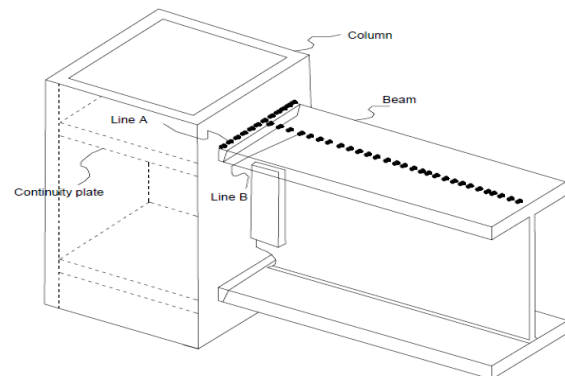


Figure 9: Critical section

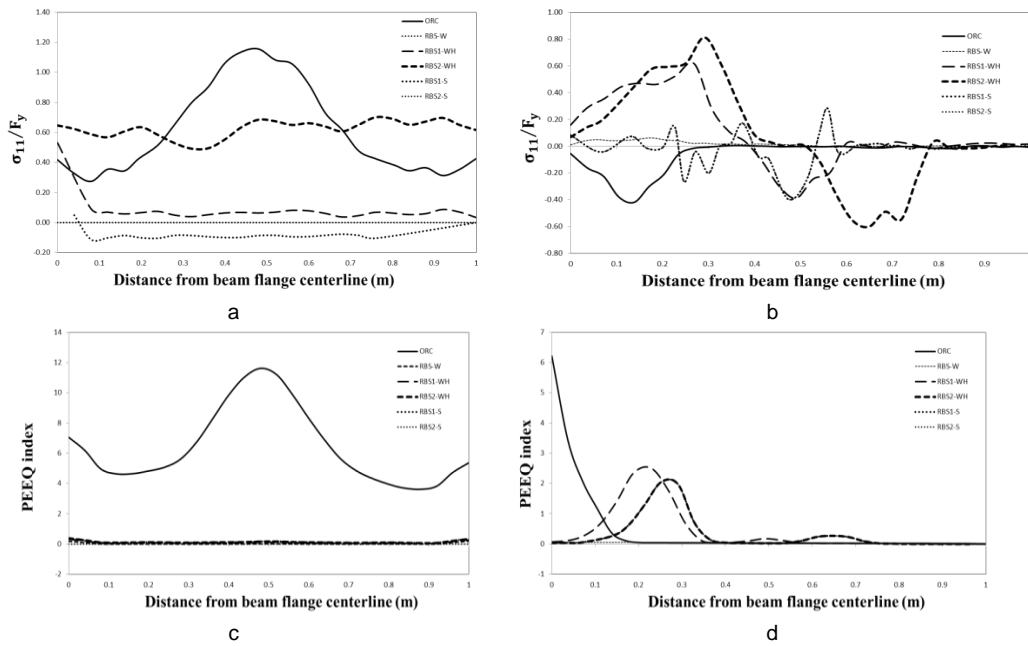


Figure 10: Longitudinal stresses and PEEQ indices at 0.06 rad rotation (a) longitudinal stresses along Line A; (b) longitudinal stresses along Line B; (c) PEEQ indices along Line A; (d) PEEQ indices along Line B.

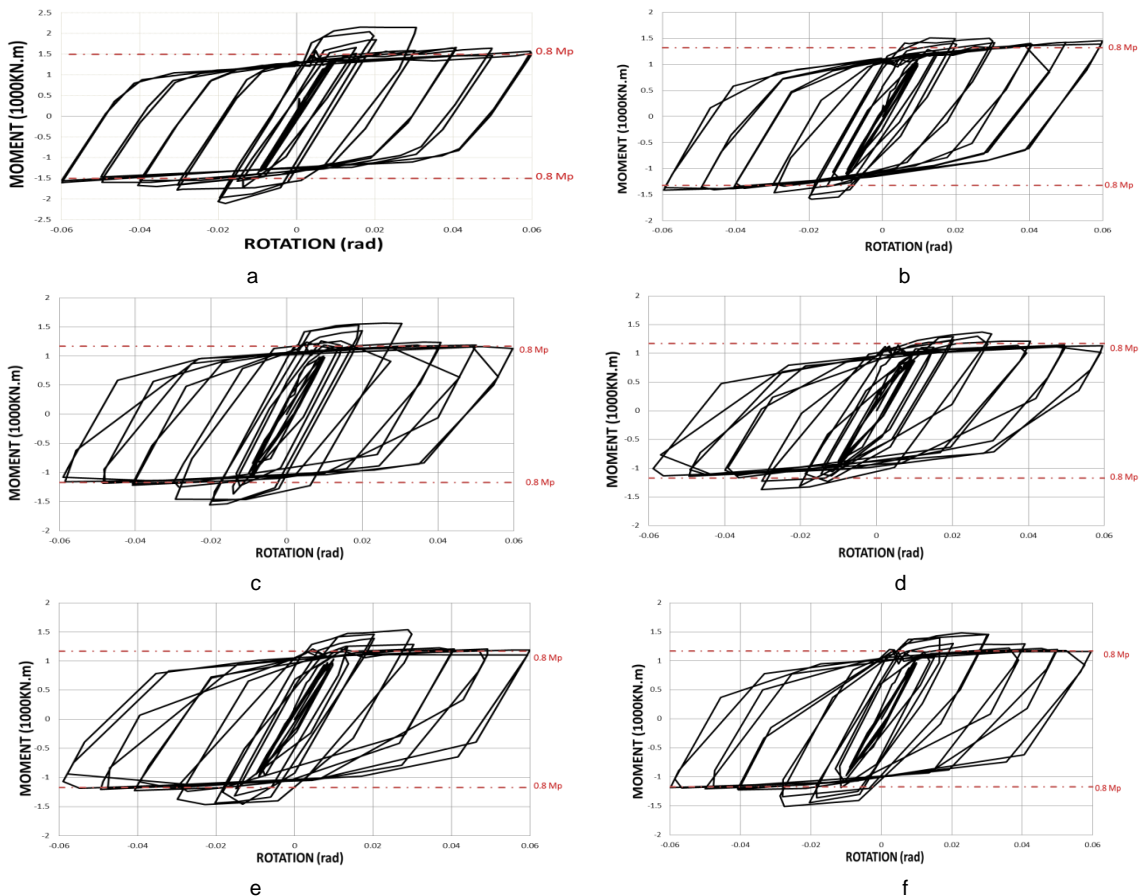
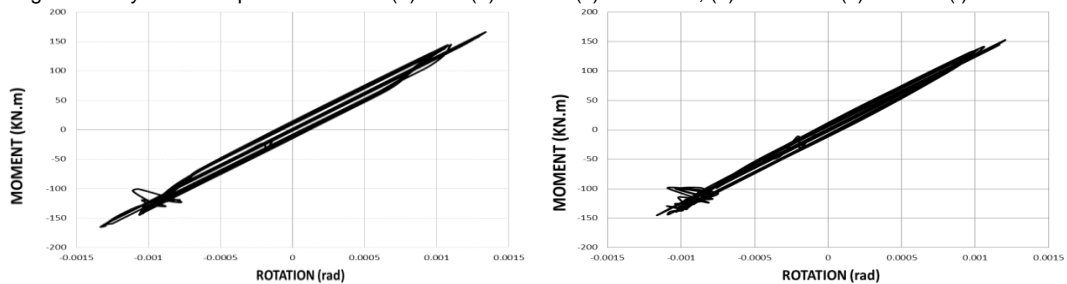


Figure 11: Hysteresis response of beam. (a)ORC (b)RBS-W (c)RBS1-WH, (d)RBS2-WH (e)RBS1-S (f)RBS2-S



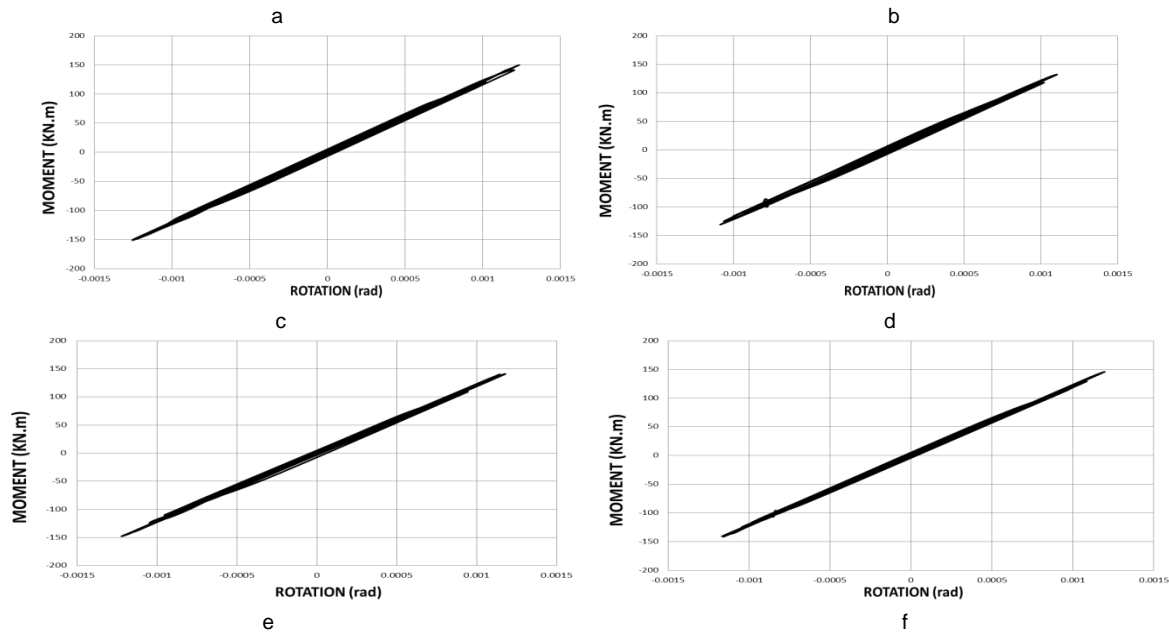


Figure 12: Hysteresis response of Panel zone. (a)ORC (b)RBS-W (c)RBS1-WH, (d)RBS2-WH (e)RBS1-S (f)RBS2-S

Table2: STIFFNESS CLASSIFICATION OF CONNECTION.

Models	$M_s$	$\theta_s$	$K_s$	$I$	$L$	$K_s L / EI$
	KN.m	Rad	KN.m	$m^4$	m	
ORC	158	0.00134	117900	197.5e-6	7.6	21.6
RBS-W	143	0.0012	119100	166.8e-6	7.6	25.86
RBS1-HW	157	0.00126	124720	197e-6	7.6	22.9
RBS2-HW	157	0.00126	124720	197e-6	7.6	22.9
RBS1-S	157	0.00125	125600	197e-6	7.6	23.07
RBS2-S	157	0.00122	128690	197e-6	7.6	23.64

### F. Dissipated Energy

The total energy dissipated by each specimen during a complete excursion of 0.06-rad total rotation is illustrated in Figure 13. The specimens RBS1-S and RBS2-S showed a slightly more energy dissipation capability compared to other reduced beam section moment connections. As observed in Figure 13, reduced beam section increases 18% of dissipated energy to compare with ordinary rigid connection.

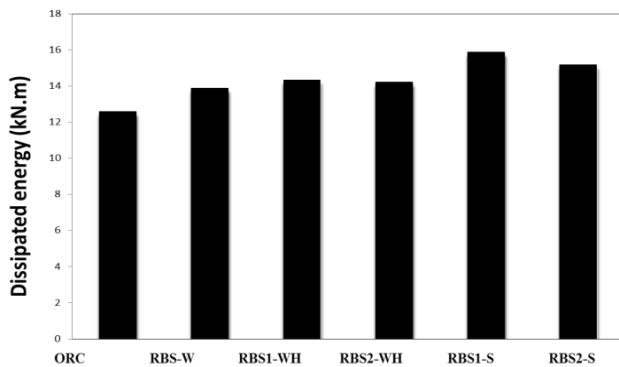


Figure 13: Energy dissipated by the whole specimen.

### CONCLUSIONS

In this paper, the obtained results from modeling by ABAQUS computer program are provided:

In the RBS connection with hole on web, plastic deformations take place significantly in the beam. Due to using reduced beam section moment connection, the panel zone in all models remains elastic. As shown in hysteretic curves, this connection is a full strength connection. This connection can be used in special moment frame (SMF) systems. Due to using reduced beam section, in moment connection, panel zone rotation is approximately 1% to 2% of total rotation therefore rotational behavior is completely independent of panel zone participation. All values of  $KL/EI$  are greater than 20, therefore this type of connection is a fully restrained connection. Reduced beam web section using sinuous holes, dissipate energy more than other types of reducing.

### REFERENCES

- [1] Engelhardt MD, Sabol TA. Reinforcing of steel moment connections with cover plates: benefits and limitations. *Engineering Structures* 1998; 20(4-6):510-20.
- [2] Engelhardt MD, Winneberger T, Zekany AJ, Potyraj TJ. Experimental investigation dogbone moment connections. *Engineering Journal, AISC* 1998;(4th quarter):128-39.

- [3] Mahin ST. (1998). Lessons from damage to steel buildings during the Northridge earthquake. *Engineering Structures*;20(4–6):261–70.
- [4] Miller DK. (1998). Lessons learned from the Northridge earthquake. *Engineering Structures*;20(4–6):249–60.
- [5] Jones, N., Wierzbicki, T., (1987). Dynamic plastic failure of a free-free beam. *International Journal of Impact Engineering* 6:240–255.
- [6] Lee CH. (2002). Seismic design of rib-reinforced steel moment connections based on equivalent strut model. *Journal of Structural Engineering*;128(9): 1121–9.
- [7] C. C. Chen, S. Wei Chen, M. Chung, M. C. Lin, (2005). Cyclic behavior of unreinforced and rib-reinforced moment connections, *Journal of Constructional Steel Research* 61 1–21.
- [8] Moslehi Tabar, A. Deylami. Promotion of cyclic behavior of reduced beam section connections restraining beam web to local buckling, *Thin-Walled Structures* 73 (2013). 112–120.
- [9] Chou, C. C., Y. J. Lai, Y. C., 2010, Seismic Rehabilitation of Welded Steel Beam-to-Box Column Connections Utilizing Internal Flange Stiffeners, *Earthquake Spectra*, Volume 26, No. 4, pages 927–950, November, Earthquake Engineering Research Institute.
- [10] Rahnavard, R. (2014). Analytical study on all type of reduced beam section moment connection affecting cyclic behavior, M.Sc. Thesis (in Persian), Institute of higher education ACECR Khuozestan, Ahwaz, Iran.
- [11] R. Rahnavard, A. Hassanipour, N. Siahpolo. (2013), Analytical study on reduce beam section moment connection effecting cyclic behavior, *Case Studies in Structural Engineering* 3 (2015) 33–51.
- [12] Chen SJ, Yeh CH, Chu JM. ( 1996). Ductile steel beam-to-column connections for seismic resistance. *Journal of Structural Engineering*;122(11): 1292–9.
- [13] [13] Stojadinovic B, Goel SC, Lee KH, Margarian AG, Choi JH. Parametric tests on unreinforced steel moment connections. *Journal of Structural Engineering* 2000;126(1):40–9.
- [14] [14] Uang CM, Bondad D, Lee CH. Cyclic performance of haunch repaired steel moment connections: experimental testing and analytical modeling. *Engineering Structures* 1998;20(4–6):552–61.
- [15] Lee CH. Seismic design of rib-reinforced steel moment connections based on equivalent strut model. *Journal of Structural Engineering* 2002;128(9): 1121–9.
- [16] Astaneh-Asl A. Seismic design of steel column-tree moment-resisting frames. *Steel tips*, Structural Steel Educational Council. 1997. pp. 40.
- [17] McMullin KM, Astaneh-Asl A. Steel semirigid column-tree moment resisting frame seismic behavior. *Journal of Structural Engineering* 2003; (9):1243–9.
- [18] Nakashima M, Inoue K, Tada M. Classification of damage to steel buildings observed in the 1995 Hyogoken-Nanbu earthquake. *Engineering Structures* 1998;20(4–6):271–81.
- [19] Lu LW, Ricles JM, Mao C, Fisher JW. Critical issues in achieving ductile behaviour of welded moment connections. *Journal of Constructional Steel Research* 2000;55(1–3):325–41.
- [20] Chen CC, Chen SW, Chung MD, Lin MC. Cyclic behavior of unreinforced and rib-reinforced moment connections. *Journal of Constructional Steel Research* 2005;61(1):1–21.
- [21] Roeder CW. General issues influencing connection performance. *Journal of Structural Engineering* 2002;128(4):420–8.
- [22] El-Tawil S, Mikesell T, Kunnath SK. Effect of local details and yield ratio on behavior of FR steel connections. *Journal of Structural Engineering* 2000;126(1):79–87.
- [23] AISC.(2005). Seismic provisions for structural steel buildings. Chicago (IL) American Institute of Steel Construction.
- [24] ABAQUS user's manual version 12.